Modeling Intraseasonal Features of 2004 North American Monsoon Precipitation

X. GAO, J. LI, AND S. SOROOSHIAN

University of California, Irvine, Irvine, California

(Manuscript received 17 October 2005, in final form 10 May 2006)

ABSTRACT

This study examines the capabilities and limitations of the fifth-generation Pennsylvania State University–National Center for Atmospheric Research Mesoscale Model (MM5) in predicting the precipitation and circulation features that accompanied the 2004 North American monsoon (NAM). When the model is reinitialized every 5 days to restrain the growth of modeling errors, its results for precipitation checked at subseasonal time scales (not for individual rainfall events) become comparable with ground- and satellite-based observations as well as with the NAM's diagnostic characteristics. The modeled monthly precipitation illustrates the evolution patterns of monsoon rainfall, although it underestimates the rainfall amount and coverage area in comparison with observations. The modeled daily precipitation shows the transition from dry to wet episodes on the monsoon onset day over the Arizona–New Mexico region, and the multiday heavy rainfall (>1 mm day^{-1}) and dry periods after the onset. All these modeling predictions agree with observed variations. The model also accurately simulated the onset and ending dates of four major moisture surges over the Gulf of California during the 2004 monsoon season. The model reproduced the strong diurnal variability of the NAM precipitation, but did not predict the observed diurnal feature of the precipitation peak's shift from the mountains to the coast during local afternoon to late night. In general, the model is able to reproduce the major, critical patterns and dynamic variations of the NAM rainfall at intraseasonal time scales, but still includes errors in precipitation quantity, pattern, and timing. The numerical study suggests that these errors are due largely to deficiencies in the model's cumulus convective parameterization scheme, which is responsible for the model's precipitation generation.

1. Introduction

This study investigated the capacity of a regional climate model (RCM) to reproduce the major elements of the 2004 North American monsoon (NAM) system. The modeling time period is from 0000 UTC 1 June to 0000 UTC 1 September, which overlaps with the North American Monsoon Experiment (NAME) 2004 Enhanced Observation Period. The NAME project aims to determine the sources and limits of predictability of warm-season precipitation over North America, and has proposed to achieve its scientific objectives by using "a symbiotic mix of diagnostic, modeling, and prediction studies together with enhanced observations" (NAME Project Science Team 2004). The current study analyzes the results of numerical modeling according to NAM system characteristics that were exposed by diagnostic studies based on historic observations and data-assimilation reanalysis. We used a currently available, physically based numerical model to check the agreement and disagreement between the model results, the statistical diagnoses, and the observations; to examine which types of features are predictable or unpredictable; and to identify the possible reasons that are associated with the model's physics. The diagnostic analysis and numerical modeling are distinct research strategies. The former is used to summarize the mean features of the NAM system based on long-term observation and reanalysis; the latter is used to simulate and predict individual NAMs under the circumstances of specific years. From the viewpoint of model improvement, it is important to examine how the diagnostic features and their variations can be captured by a numerical model in its case-by-case predictions. This study intends to evaluate the fifth-generation Pennsylvania State University–National Center for Atmospheric Research Mesoscale Model's (MM5) capabilities and limitations in reproducing intraseasonal vari-

Corresponding author address: Xiaogang Gao, CHRS, Dept. of Civil and Environmental Engineering, University of California, Irvine, Irvine, CA 92697.
E-mail: gaox@uci.edu

DOI: 10.1175/JCLI4100.1

abilities in the NAM precipitation in the context of the 2004 monsoon season.

Studies for the past two decades have significantly improved the description and understanding of the NAM system. This includes identifying and clarifying spatially and temporally coherent relationships among the interactive physical variables of the ocean, atmosphere, and land surface. Among the most important diagnoses are the following:

1) the NAM system's synoptic- dynamic, and thermodynamic, mechanisms; including its circulation characteristics and their spatial and temporal variations (Douglas et al. 1993; Adams and Comrie 1997; Barlow et al. 1998; Higgins et al. 1997);
2) the ENSO–NAM precipitation relationship and NAM interannual variability (Ropelewski and Halpert 1996; Higgins et al. 1999; Higgins et al. 2000);
3) onset and northward extension of NAM precipitation and the "tripole" interaction among summer precipitation regimes over the continental United States (Higgins et al. 1999; Mo 2000);
4) moisture surges over the Gulf of California and the low-level jet (LLJ) from the northern end of the gulf to the southwest United States (Stensrud et al. 1997; Anderson et al. 2000; Douglas and Leal 2003; Higgins et al. 2004; Saleeby and Cotton 2004); and
5) diurnal variability of convective rainfall and low-level flow over the NAM region (Stensrud et al. 1995; Douglas and Li 1996; Douglas et al. 1998; Li et al. 2004).

These well-documented findings provide guidance for this modeling study's understanding and prediction of the NAM. Because the numerical experiments are restricted to the core NAM region of the southwestern United States and northern Mexico, the 2004 NAM results are examined in diagnoses 3–5 above.

It is well known that the results of a regional climate model can be affected by many factors, including the selection of the modeling configurations, boundary forcing, initialization data, and methods. One decision that must be made for modeling the 2004 NAM is how frequently the model run should be adjusted (by reinitialization or nudging methods) using observation data assimilations to restrain the error growth and keep the simulation in line with reality. Two approaches have been employed, depending on particular modeling objectives. Studies to simulate the processes of a specific NAM usually were updated frequently, for example, every 12 h (Stensrud et al. 1995), daily (Stensrud et al. 1997), or every 2 days (Saleeby and Cotton 2004). While such frequent adjustments enable the model to trace observations closely, it is difficult to evaluate the model's ability to predict dynamic processes beyond the updating (time) interval. The second widely employed approach is to update a model run once a month or longer (Gochis et al. 2002; Liang et al. 2004; Li et al. 2004; Xu et al. 2004). However, these approaches perform poorly in simulating short-term processes and are used mostly to analyze the NAM's monthly or seasonal mean features. Following the first approach in the 2004 NAM modeling and through a set of pretests, we found that by reinitializing every five model days—the longest updating time interval in our tests, the 2004 NAM simulation was comparable with observations and consistent with the NAM's diagnostic features when checked at intraseasonal time scales (i.e., the monthly to daily means). Because predicting intraseasonal precipitation and circulation features is an important issue for operational short-term weather/climate forecasts and because the predictions have many applications, to areas such as hydrology and agriculture, we focus on examining the model's performance in reproducing important intraseasonal features of the 2004 NAM.

2. Model description

The model for this study is version 3 of MM5. The model setting and the selected physics schemes are as follows.

1) *Domains and grids:* Two domains are nested inside the European Centre for Medium-Range Weather Forecasts (ECMWF) global 2.5° grid system, as shown in Fig. 1. Domain 1 (close to NAME tier 3) covers the conterminous United States, Mexico, and a portion of the tropical region with a 75-km horizontal grid. Domain 2 (close to NAME tier 2) includes the southwestern United States and Mexico, with a 25-km grid to represent the region's complex topography. The vertical coordinate is a terrain-following σ system. The 28 vertical σ layers are used from the surface to the top of the atmosphere (100 mb) with 10 layers below 700 mb.
2) *Lateral boundary forcing and model initialization:* The ECMWF global TOGA 2.5° × 2.5° analysis data (available for 1985 to the present) from June to August 2004 were used for model lateral boundary forcing and internal grid initialization. The lateral forcing along the border of domain 1 was updated every 12 h, and the model initialization was at 1200 UTC every 5 days throughout the entire simulation period. Each reinitialization includes an additional 12-h model run for spinning up.

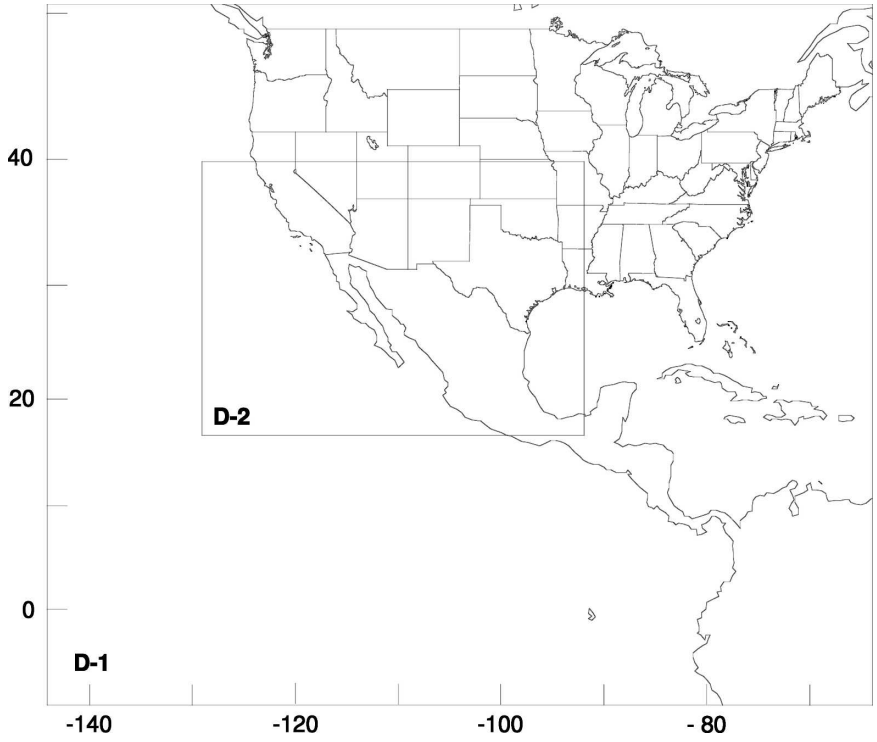

FIG. 1. The study domains.

3) *Sea surface temperature (SST):* The newly developed Moderate Resolution Imaging Spectrometer (MODIS)/*Aqua* SST data (available online at http://modis-ocean.gsfc.nasa.gov) with weekly and 4.63-km resolutions are used to force the oceanic boundary. The use of high-resolution SST data is expected to improve the description of SST variations in the Gulf of California and eastern Pacific Ocean, which, as shown by previous studies (Gao et al. 2003; Li et al. 2005), plays an important role in NAM modeling.
4) *Physics schemes:* At the selected spatial resolution (25 km) over the core NAM region, monsoon rainfall is produced largely by the convective parameterization scheme. This study uses the Kain–Fritch (K–F) cumulus convective parameterization scheme (Kain and Fritch 1990). Previous studies indicate that the K–F scheme works well at a spatial resolution of 25 km and performs better than other schemes over the NAM regions (Wang and Seaman 1997; Stensrud et al. 1997; Gochis et al. 2002). Other physics schemes used in the study include the simple ice explicit moisture adjustment scheme (Dudhia 1989), the cloud radiation scheme (Dudhia 1989), and the Noah land surface model (Chen and Dudhia 2001).
5) *Planet boundary layer (PBL) scheme:* The boundary layer description is critical for monsoon precipitation simulation (Bright and Mullen 2002). Our test experiments indicate that the Medium-Range Forecast (MRF) boundary layer scheme (Hong and Pan, 1996) works relatively well over land but will overestimate tropical rainfall, while in comparison to the MRF scheme, the Eta Model PBL scheme (Janjić 1994) produces more reasonable tropical rainfall but overestimates rainfall over the extratropical oceanic region. Because tropical rainfall can influence NAM system development significantly (Yu and Wallace 2000; Higgins and Shi 2001), this study uses the Eta PBL scheme in domain 1 (which includes a portion of the Tropics) and the MRF scheme in domain 2, with one-way communication between these domains.

3. Precipitation observation data

Three precipitation observation datasets are used to evaluate the model's precipitation output.

1) *National Centers for Environmental Prediction (NCEP) 0.25° grid rainfall data* (hereafter the NCEP gauge data): The NCEP gauge data (information available online at http://www.cpc.ncep.noaa.gov/products/precip) are interpolated from daily rain gauge measurements over the United States and

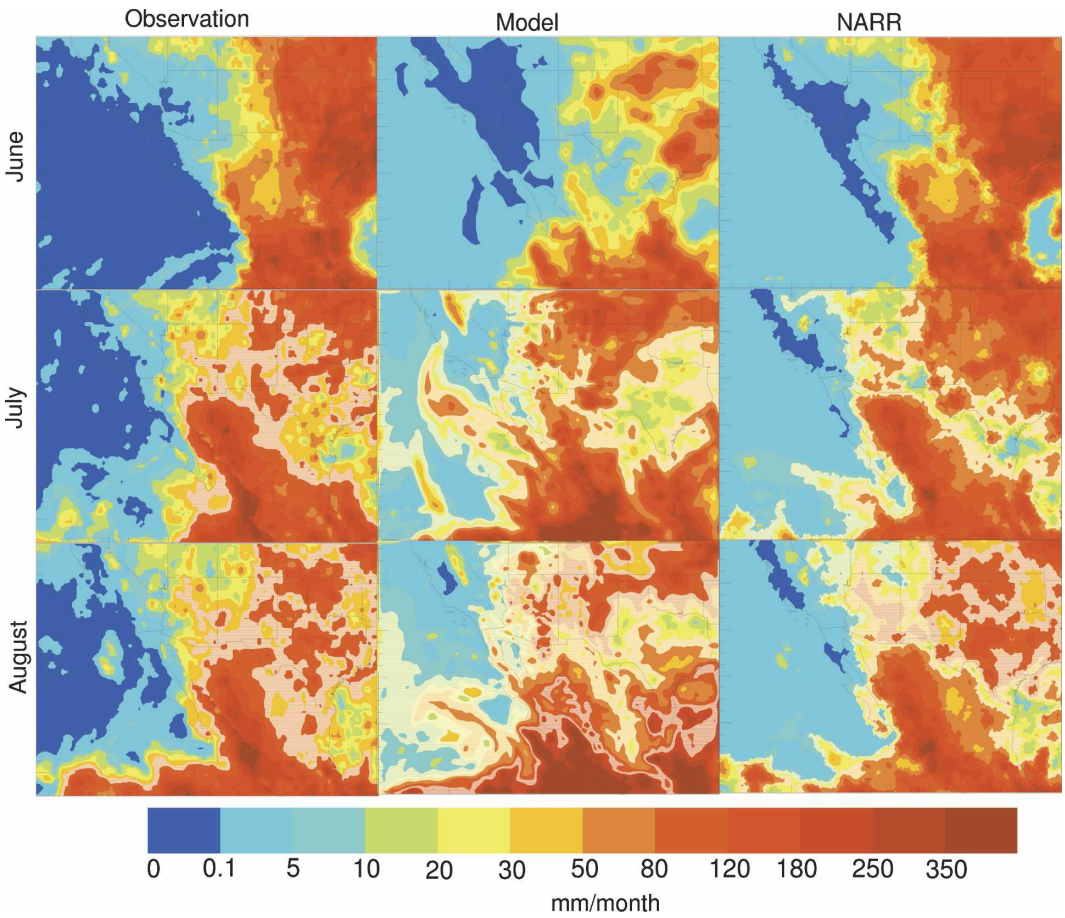

FIG. 2. Comparison of monthly precipitation using (left) the NCEP gauge data over land and the PERSIANN estimates over oceans, (middle column) the MM5 simulations, and (right) the NARR, in (top) June, (middle row) July, and (bottom) August 2004.

Mexico and have been used in many NAM studies. In the mountainous core NAM region, the NCEP rain gauges are sparse and heterogeneous, with more gauges located in the accessible areas than on the mountains, which will cause an underestimation of precipitation over the mountains.

2) *NAME Event Rain Gauge Network (NERN):* To produce an intensive observation of NAM precipitation over the NAM core area (tier 1), the NAME project has built the NERN gauge network in northwestern Mexico. This network was installed during 2002 and 2003, and includes 81 gauges divided into six west–east transects (T1–6) across the western slope of the Sierra Madre Occidental between 22° and 30°N (Gochis et al. 2003, 2004). The guiding principle for installing the NERN is to improve sampling of precipitation variability along the regional topographic gradients.
3) *Precipitation Estimation from Remotely Sensed Information using Artificial Neural Network (PERSIANN):* The recent version of the PERSIANN data provides hourly 4-km precipitation estimates based on cloud infrared and microwave imagery from multiple satellites (Hsu et al. 1997; Sorooshian et al. 2000; Hong et al. 2004). One unique feature of satellite precipitation data is that it can monitor the distribution and evolution of NAM rainfall over the Pacific Ocean. However, satellite-based data on surface rainfall are estimated indirectly from the cloud images, and their rain-rate estimates can be affected by many factors (Sorooshian et al. 2000).

4. Results

a. Precipitation evolution

Figure 2 compares the observed, modeled, and reanalysis monthly rainfall fields in the NAM region. In the observations, precipitation over land is from the NCEP gauge data, and precipitation over the oceans is from the PERSIANN estimates. The NCEP–National

Center for Atmospheric Research (NCAR) Regional Reanalysis (NARR) data are produced with reinitializations every 2.5 days (with an additional 12-h run for spinning up) and also leveraged by frequent three-dimensional observation data assimilation (3DDA) including precipitation and many other physical variables (Mesinger et al. 2005). For the use of 3DDA, the daily NCEP gauge data over land and the (satellite based) Climate Prediction Center (CPC) Merged Analysis of Precipitation pentad data over oceans are disaggregated into hourly values. Figure 2 shows that the reanalysis and the observation monthly rainfall are highly correlated. By ingesting observation data into the modeling, the reanalysis data aim at capturing the regional meteorological and hydrological features of the weather and climate systems. As mentioned above, the MM5 modeling is operated under the conditions of every fifth-day reinitiations and without using observation data assimilation. In general, the model reproduces the monsoon precipitation characteristics in the three summer months over land. However, over the eastern Pacific Ocean, the model generates excessive precipitation, mainly because the use of the Eta PBL scheme in domain 1 that is known to produce unrealistic rainfall predictions in the subtropical oceanic region (see above) and to affect domain 2 through the west boundary. Over land, the model illustrates the evolution characteristics of the monsoon rainfall, matching the summary based on observations (Douglas et al. 1993; Higgins and Shi 2001; Cavazos et al. 2002). In June, rainfall is concentrated on a band from southern Mexico along the coastal line of the Gulf of Mexico to the Great Plains. Meanwhile, the model shows that monsoon rainfall starts growing northward along the western slope of the Sierra Madre Occidental (SMO). Arizona is dry in June. In comparison with the observations, the model underestimates not only the major rainband in northeastern Mexico, Texas, and the Great Plains, but also NAM rainfall over the western coast of Mexico. In July, although the model still underestimates rainfall, it shows that the NAM precipitation regime reaches northwestern Mexico and continues extending northeastward, passing Arizona and New Mexico into the high plains of Colorado and Kansas. In contrast, the rainfall band along the coastal line of the Gulf of Mexico to the Great Plains declines. In August, monsoon precipitation becomes weak along the western coast of Mexico, but continues growing in Arizona. Meanwhile, precipitation over northeastern Mexico, Texas, and the Great Plains regains strength compared with the decline in July.

These monthly precipitation variations are associated with the synoptic progression of circulations over the conterminous United States and Mexico, as described by the diagnostic studies cited above. Figure 3 presents the differences among 200-mb streamlines, 850-mb wind vectors, and precipitation over land in two consecutive months. From June to July (Fig. 3a), the changes in the upper-tropospheric winds (200-mb streamline) show a pattern similar to that derived from the long-term composition of NCEP–NCAR reanalyses (Higgins et al. 1999, their Fig. 8c): a broad cyclone over the north-central United States and east-to-west streamlines over the tropical region, which indicates the monsoon anticyclone's northward migration from southern Mexico in June to the vicinity of northwestern Mexico by July. At the 850-mb level, the model shows typical NAM low-tropospheric wind variations, including an increase in the tropical westerly, a decrease in the southerly over the Gulf of Mexico and the Great Plains, and a decrease in the northwesterly west of Baja California. Correspondingly, the precipitation pattern illustrates "tripole" interactive relationships: an increase (exceeding 1 mm day^{-1}) over the NAM region, an out-of-phase decrease over the Great Plains/northern tier, and an in-phase increase over the eastern United States.

The circulation and precipitation changes from July to August (Fig. 3b) reveal pronounced reverse patterns in comparison with the June–July variations, which are also similar to the NCEP–NCAR reanalysis compositions (Higgins et al. 1999, their Fig. 8c) and indicate that the NAM grows from maturity to decline. At 200 mb, an anticyclone replaces the cyclone in the subtropical U.S. region, with tropical streamlines running in the opposite direction, indicating "a tendency of the monsoon anticyclone to begin its southward track" (Higgins et al. 1999). The 850-mb winds show the strengthening of the tropical easterly and the Pacific northwesterly (west of Baja California). The Great Plains and the eastern United States experience complicated local wind variations. Surface precipitation variations are correlated with these circulation changes. The monsoon rainfall regime decays except for northwestern Mexico, Arizona, and southern Nevada, where NAM precipitation continues growing. Meanwhile, over northeastern Mexico, Texas, and Great Plains, precipitation strengthens to the west and weakens to the east. Over the eastern United States, precipitation decreases in the northern region but increases in the southern and coastal regions. Over southern Mexico, the RCM predicts increased rainfall in August, in contrast with the decrease observed from the NCEP gauge data (not shown). This positive bias in model precipitation is associated with the synoptic circulation and with the model's deficiencies in overestimating tropical rainfall. During the

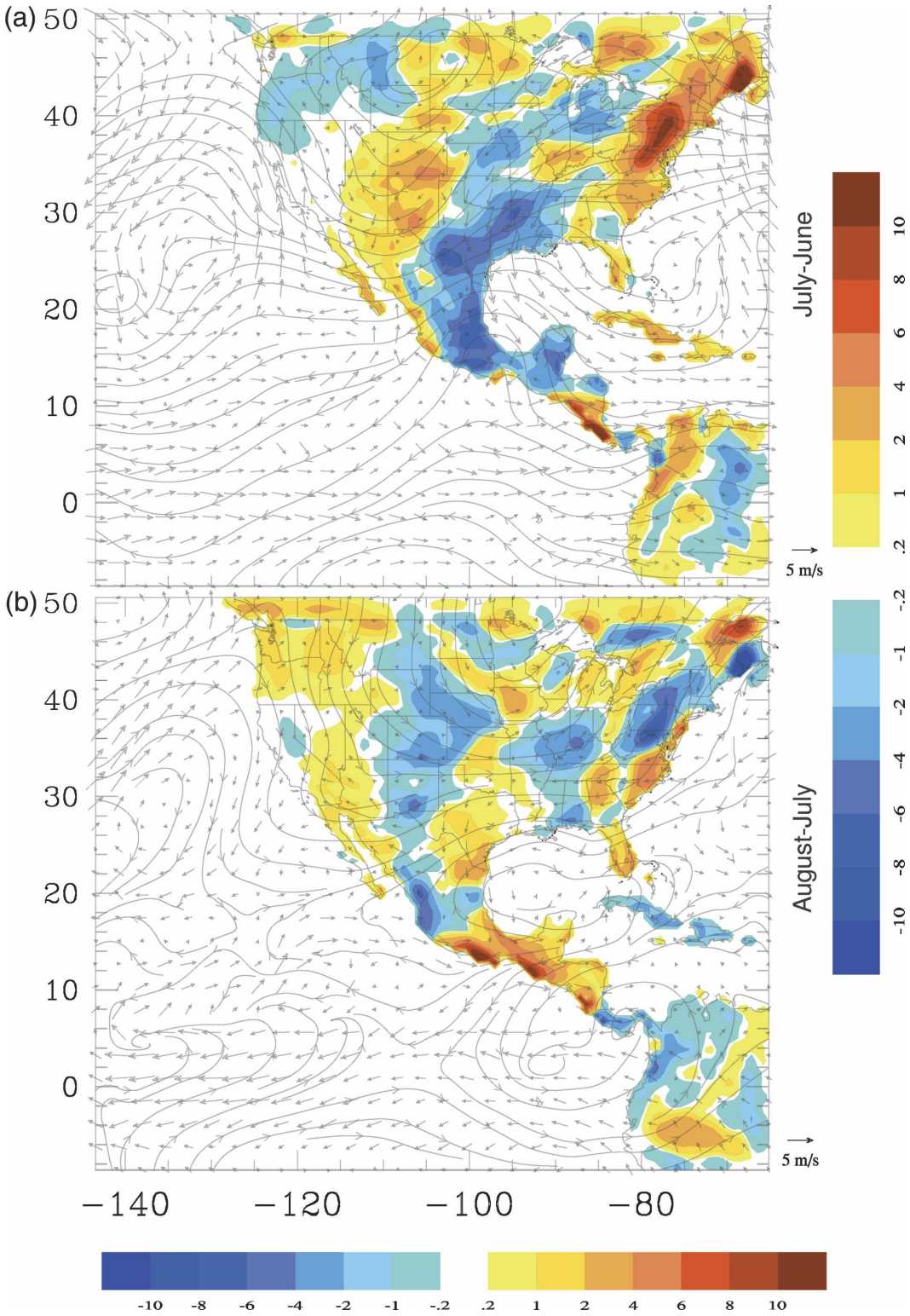

FIG. 3. Differences in modeled 200-mb streamlines, 850-mb wind vectors, and precipitation between two consecutive months: for (a) July−June and (b) August−July.

NAM's mature period, the subtropical high (near the plateau) dominates southwestern North America and results in the prevalence of warm southerly winds from the tropical Pacific over southern Mexico. This synoptic pattern predisposes the model to produce rainfall over the region (Li et al. 2004).

In diagnostic studies, the date of monsoon onset is found to be a useful indicator to estimate many important features (strong–weak, wet–dry) of the coming monsoon and winter (Higgins et al. 1997; Higgins and Shi 2000). Based on historic observational data, Higgins et al. (1997, 2000) have defined the monsoon onset date for the southwestern United States as the first day after June 1 when the daily mean precipitation over the Arizona–New Mexico (AZNM) region (32°–36°N and 112.5°–107.5°W; see Fig. 1) exceeds 0.5 mm day^{-1} for three consecutive days. The time series of daily precipitation over the AZNM region in Fig. 4a shows a dry June, and a wet July and August. The model predicted two rain events during 23–30 June that exceeded 0.5 mm day^{-1} and lasted for 3 days. However, the observational data show that both rainfall events have much smaller amounts and shorter durations, thereby refuting the premise about the 2004 NAM onset. If we exclude these two rainfall events in June, the model and observational data agree upon 11 July as the onset day. After the monsoon onset, the observational data show that the AZNM region experienced a continuous "wet episode" that included four heavy rain (>1 mm day^{-1}) intervals: 11–19 and 23–29 July, and 2–7 and 13–20 August. The model time series shows the same dry-to-wet transition on 11 June, as well as the four heavy rain intervals in 11–19 and 23–28 July, 31 July–7 August, and 13–17 August. Clearly, although the model predictions show errors in rainfall amounts and timing, they nonetheless capture the critical diagnostic intraseasonal features of precipitation over the AZNM region.

Figure 4 plots the time series of modeled and observed daily rainfall over five 2° × 2° boxes along the southwestern United States and northwestern Mexico (see Fig. 1 for locations). The five boxes are located at

A (33°–35°N, 108°–110°W)—Mogollon Rim on the Arizona–New Mexico border;
B (32°–34°N, 111°–113°W)—Sonora Desert in southwestern Arizona;
C (28°–30°N, 108°–110°W)—Sonora, northwestern Mexico;
D (24°–26°N, 106°–108°W)—Sinaloa, western Mexico; and
E (20°–22°N, 102°–104°W)—west-central Mexico.

The observational data on rainfall over boxes A and B (inside the AZNM region) shows that the model generated three unrealistic heavy rainfall events in June in box A, the Mogollon Rim (not in box B, Sonora Desert). The last two events raise the mean rainfall intensities over the AZNM region to greater than 0.5 mm day^{-1} for 3 days, which could lead to misidentification of the monsoon onset date, as discussed above. This problem is due to the K–F convective parameterization scheme, which tends to predict excessive precipitation over mountains (Wang and Seaman 1997; Liang et al.

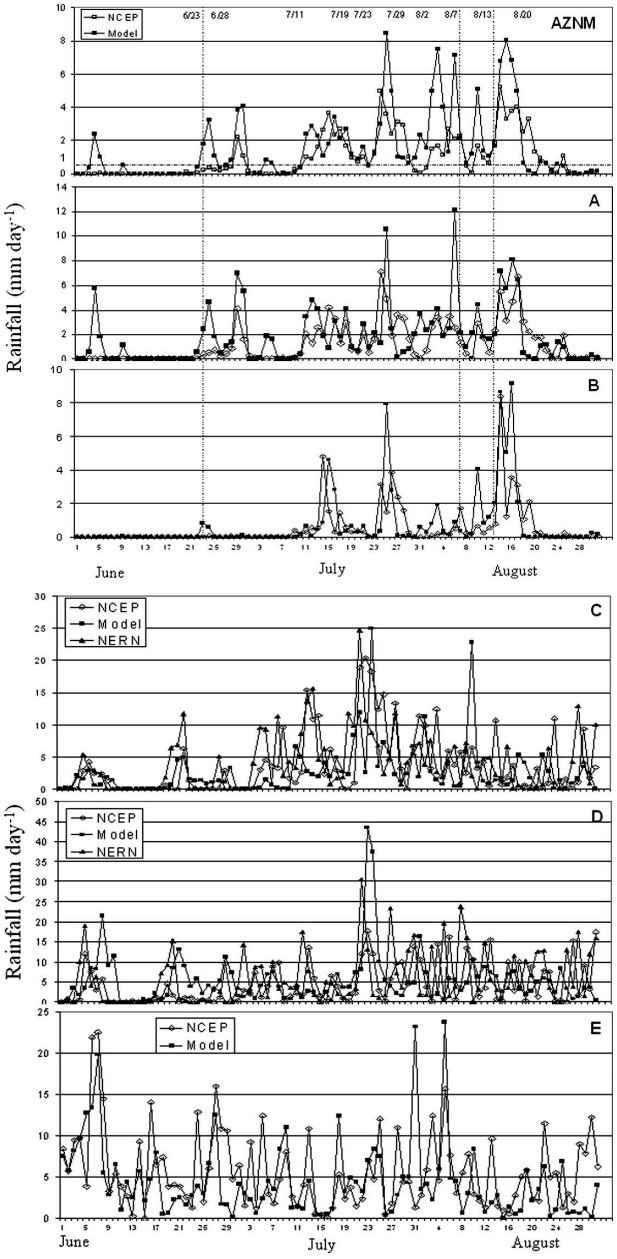

FIG. 4. (a) Time series of observed and modeled daily precipitation from 1 Jun to 31 Aug 2004, over the AZNM, A, and B boxes. (b) The same as in (b) but for boxes C, D, and E.

2004). In July and August, the model showed four major rainy periods in box A and three in lower-elevation box B that generally matched the observations.

Boxes C and D are located in the NAME intensive field observation area. Box C covers 23 NERN rain gauges from the T5 and T6 transects, and box D includes 12 NERN gauges from the T2 and T3 transects. The precipitation observations from both the NCEP gauge data and the NERN gauge network are plotted in Fig. 4b (NERN, lines with triangles; NCEP, lines with diamonds). These observations are highly correlated with each other, but the NERN daily rainfall often seems higher and earlier (~1 day) than that observed from the NCEP gauge data. The PERSIANN satellite rainfall estimates over the boxes more closely match the timing of heavy rainfall observed from the NERN network than do the NCEP gauge data (not shown). This is because the NERN network has installed many rain gauges in high-elevation areas in regions indicated by the boxes, while the NCEP gauges are concentrated largely in accessible low-elevation areas. The mountain areas receive more rainfall at an earlier time than the low-elevation areas (see the discussion in section 4c). Monsoon rainfall over boxes C and D starts earlier and is much heavier, with more variability than the rainfall over boxes A and B. The model seems to lack agility in simulating such quick variations, resulting in precipitation underestimation.

Box E represents the area in the south of the Gulf of California and a portion of inland west-central Mexico. The simulation traced the observed rainfall perturbations in general, but missed many severe rainfall events.

b. Moisture surge over the Gulf of California

The moisture surge over the Gulf of California is an important intraseasonal feature of the NAM system. Previous studies indicate that most moisture for monsoon rainfall in the southwestern United States is transported from the tropical Pacific through surges (Adams and Comrie 1997; Stensrud et al. 1997; Anderson and Roads 2002; Douglas and Leal 2003; Higgins et al. 2004). Douglas and Leal (2003) identify the conditions to define a surge based on radiosonde data at Empalme, Mexico. Higgins et al. (2004) introduce diagnostic criteria to identify surges occurring over Arizona based on surface meteorological observations at Yuma, Arizona:

(a) dewpoint temperature from below the climatological mean [15.7°C (60.1°F)] to higher than the mean and sustained for at least three consecutive days,
(b) wind (at 700 and 200 hPa) speed exceeds the climatological mean (>4 m s^{-1}) and remains elevated for a few days (a week or more for strong surges), and
(c) wind direction from northerly to southerly.

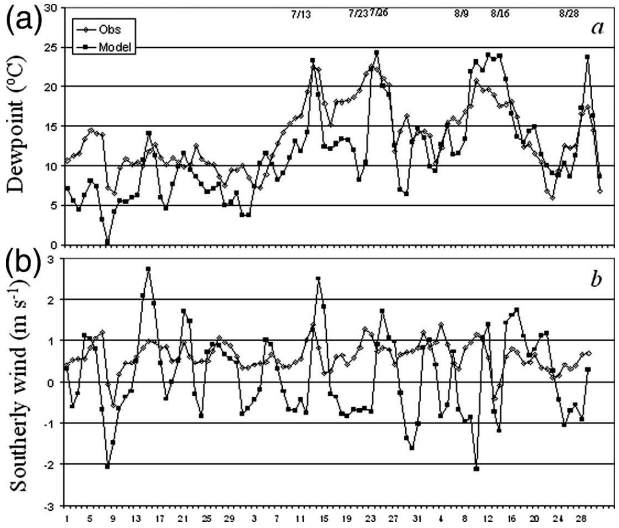

FIG. 5. Time series of observed and modeled daily (a) surface dewpoint and (b) 10-m meridional winds at Yuma.

In Fig. 5, the modeled daily dewpoint and meridional wind at 10-m height in the grid box that covers Yuma are plotted with the corresponding surface observation data at the Yuma Valley station (information online at http://ag.arizona.edu/azmet/). The observational data from the other two stations, Gila and Mesa, were checked, and they are almost identical to the data at Yuma Valley. The ground observation data enable the identification of four surges during July and August: surge 1, 11–15 July; surge 2, 17–26 July; surge 3, 8–16 August; and surge 4, 28–30 August. Correspondingly, the surges determined from the model data are as follow: surge 1, 13–14 July; surge 2, 23–26 July; surge 3, 9–16 August; and surge 4, 28–29 August. Both surges 1 and 2 are identified with different onset dates and durations when using modeled and observed data. The cause of the differences was investigated using the diary of the "NAME Previous Day Summary," written by the NAME committee members (available online at http://www.joss.ucar.edu/cgi-bin/catalog/name), during the NAME intensive observation period. The diary's summary reported that on 11 July, "Dewpoint at 12Z [0000 UTC] remained in the low to mid 50's across southern AZ" and on 13 July, "Flow in the Gulf of CA had increased from the south setting up what will most likely become Gulf Surge #1. At 12Z, the dewpoint at Yuma had increased to 70." Apparently surge 1 started on 13 July, which agrees with the model prediction. After 14 July, the summary recorded no surge until 23

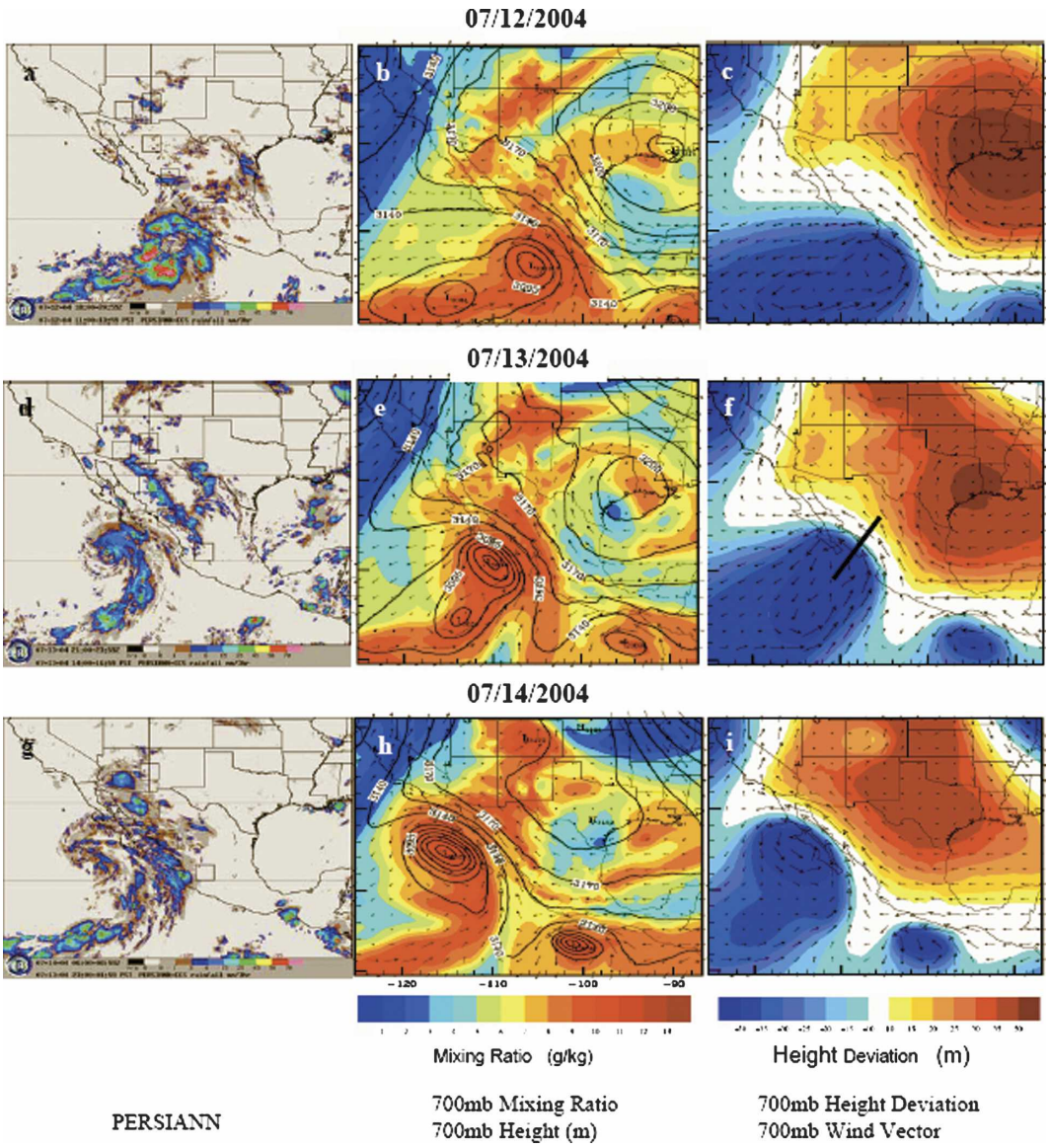

FIG. 6. Progression of surge 1 stimulated by Tropical Storm Blas on (top) 12, (middle row) 13, and (bottom) 14 July with the Blas positions traced by the (left) PERSIANN rainfall estimates, (middle column) 700-mb geopotential height and mixing ratio, and (right) 700-mb wind and geopotential height deviation from the area mean.

July, when it reported that "Tier 1 is under a strong gulf surge." Again, the model onset date for surge 2 is correct. The model seems to work well in predicting 2004 NAM surge events. We suspect that the ground measurements of daily dewpoint and winds in the dataset may not be reliable because a large amount of missing data was found in the files for these variables possessing high diurnal variations. Therefore, one should be cautious about using ground observation data to identify surge onset and ending dates for the NAM.

Anderson et al. (2000) have identified two types of surges: 1) tropical cyclone surges, which are associated with the passage of tropical disturbances (such as hurricanes and tropical storms) to the south of Baja California, and 2) easterly trough surges, which are associated with the westward propagation of a low-level trough from the SMO to the eastern Pacific. Surge 1 was clearly a tropical cyclone surge. On 12 July, Tropical Storm Blas was moving northward near the mouth of the Gulf of California, and surge 1 started on 13 July. Figure 6 displays the progression of surge 1 in 700-mb mixing ratio, geopotential height deviation, wind, and geopotential height on 12–14 July, accompanied by the PERSIANN rainfall, which shows Blas's migration.

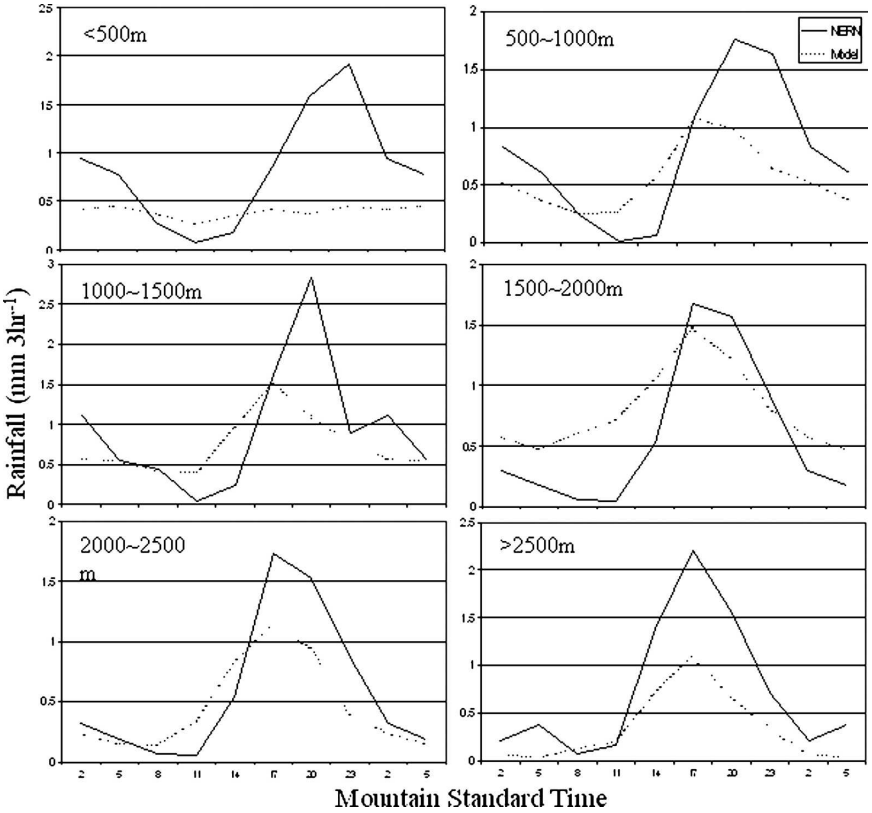

FIG. 7. Observed (NERN) and modeled mean diurnal precipitation cycles in July at six elevation bands across the western slope of the SMO.

The model's description of the surge event agrees with previous studies. In Fig. 6, the isobars of 700-mb height (middle column) delineate the movements of the cyclone Blas and the monsoon anticyclone. When the cyclone moved northward to the gulf and dispersed west of southern Baja California, the anticyclone moved westward from Louisiana to central Texas. During the surge period, over the Gulf of California, southeasterly winds strengthened (right column) and moisture became concentrated (middle column). The initiation of the surge event started on 13 July (Fig. 6f) when Blas brought strong pressure-gradient forcing near the mouth of the gulf, resulting in a surge front that propagated through the gulf over a span of 18–30 h (Stensrud et al. 1997). Once the surge front passed, the southeasterly winds over the gulf continued for another day. The winds were maintained (Fig. 6i) by a geostrophic balance between a low pressure center located to the southwest of the gulf and a high pressure area situated over the SMO (Anderson et al. 2000). Figures 6b, 6e, and 6h (middle column) show that in the surge event, a large amount of moisture accumulated over the gulf and northern Mexico, then spread to Arizona, New Mexico, and southern Colorado. When this paper was prepared, we were unable to find the NAME field measurement data (as well as the NARR data) to evaluate the modeled surge processes (therefore, we will not discuss the model results for other surge events). When the observation field data and reanalysis data are available they should provide the basis for an interesting future study.

c. Diurnal variability of precipitation and low-level flow

Evidence from satellite and ground observations as well as model simulations demonstrates that NAM rainfall is strongly modulated by diurnal variations (e.g., Negri et al. 1993; Dai et al. 1999; Sorooshian et al. 2002; Berbery 2001; Mo and Juang 2003; Li et al. 2004). Based on hourly data from the NERN gauge network, Gochis et al. (2004) found that diurnal cycles of precipitation frequency and intensity have distinct relationships to terrain elevation. Figure 7 compares the 3-hourly rainfalls of July at six elevation bands (bins) along the western slope of the SMO with the NERN observations. The model results demonstrate pronounced diurnal cycles, but exhibit two major errors in comparison with the NERN results: 1) the model diur-

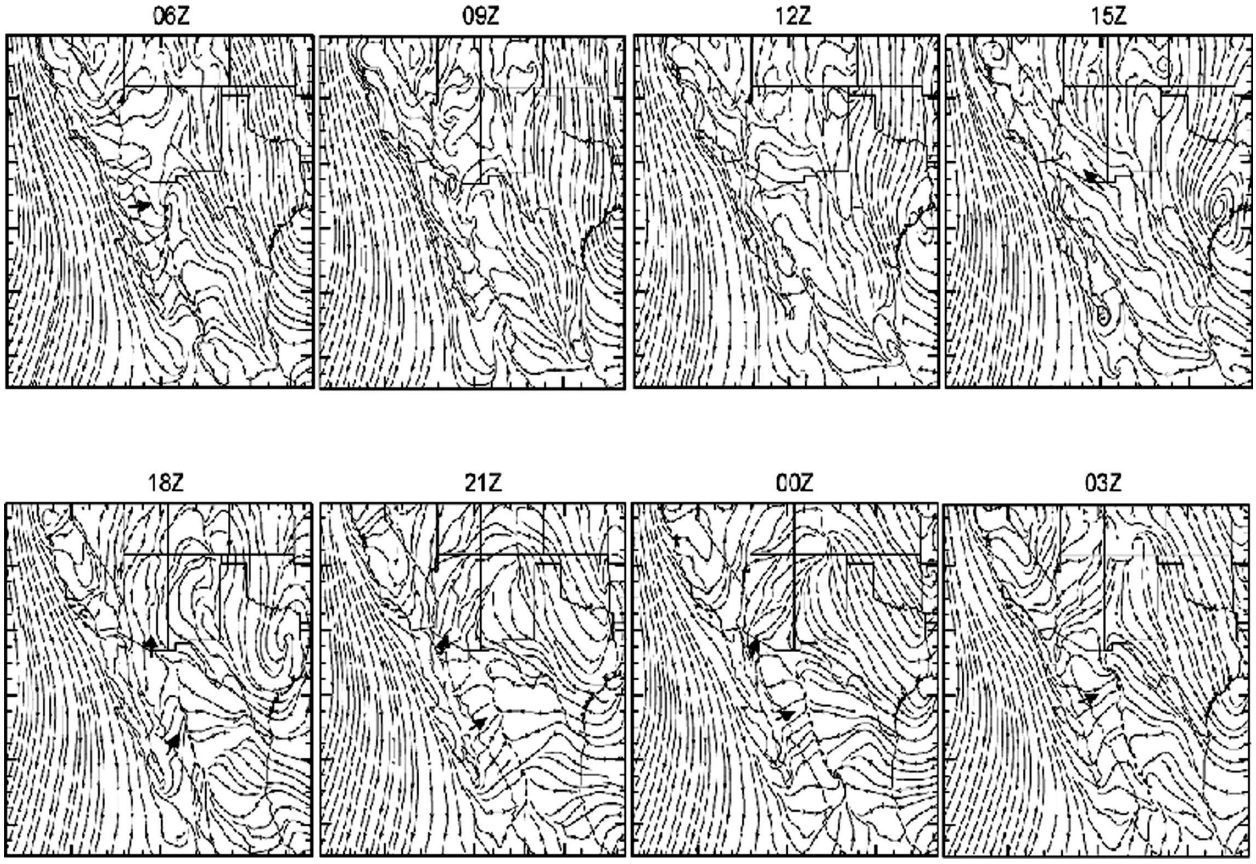

FIG. 8. Mean diurnal variations of surface streamlines (low-level flows) in July over the core NAM region times are UTC with 06Z = 0600 UTC etc.

nal cycles at all elevations except the lowest (elevation <500 m) share a similar diurnal phase variability, with peak rain occurring at around 1700 mountain standard time (MST). In contrast, the observed diurnal cycles across the SMO slope show a shift in diurnal peak from local afternoon (~1700 MST) over the highest elevation to late evening (~2300 MST) over the lowest, and 2) the model underestimates the diurnal peak intensity over all elevation bands. In particular, the model rainfall over the lowest-elevation band (<500 m) shows a low and flat distribution throughout the period of a day without visible diurnal variability, which differs from the observed diurnal variability with its late evening peak.

To understand the cause of the diurnal precipitation feature over the western slope of the SMO, Fig. 8 presents 3-hourly diurnal patterns of the streamline in July at $\sigma = 0.9535$ (~500 m above the terrain surface). From local late morning (1100 MST or 1800 UTC) to later night (2300 MST or 0600 UTC), sustaining sea breezes from the Gulf of California and the eastern Pacific invade western Mexico and bring rich moisture to the western slope of the SMO. During this period, the convergence line (the dotted lines) of the lateral flows shifts from near the SMO peak (the Continental Divide) to near the coastline. The convergence line indicates the location where vertical motion or convection occurs. Therefore, the model does predict a migration of convection activity from local afternoon over the highest-elevation band to late night over the lowest-elevation band, which matches the observed shift of the rain peaks. The well-simulated convection migration (the convergence line) over the SMO's west slope suggests that the errors in diurnal rainfall cycles result from a deficiency in the convective parameterization scheme.

Figure 8 shows that in the morning [0500–1100 MST (1200–1800 UTC)], instead of producing westward land breezes across the coast to the Gulf of California, the low-level flows turn to southeasterly winds. A low-level jet (LLJ) from northern Mexico across the Mexico–U.S. border in Arizona and New Mexico reaches the southwest United States [Fig. 8 at 0800 MST (1500 UTC)], bringing moisture to the region. In the afternoon and night [1400–2300 MST (2100–0600 UTC)],

another LLJ from the northern end of the gulf flows into Arizona. This LLJ is considered the major moisture source of monsoon rainfall in the southwestern United States (Stensrud et al. 1995; Douglas and Li 1996; Anderson et al. 2000). However, based on observations at Yuma, Arizona, Douglas and Li (1996) have determined that the timing of the maximum LLJ from the northern Gulf of California occurs in the early morning hours (1200 UTC), not in the afternoon, as the model shows. This has been one of the key research issues in the NAM modeling study. The results of Saleeby and Cotton (2004) are comparable to ours. The modeling of Anderson et al. (2000) shows that the LLJ occurs over the western portion of the northern gulf and the foothills of the SMO at 1200 UTC, then extends across the gulf at 0000 UTC. Stensrud et al. (1997) show that LLJ development is related to the moisture surge over the Gulf of California. Figure 8 demonstrates that the core NAM region of northern Mexico and the southwestern United States is between two synoptic flows with opposite directions: the northwesterly, from the eastern Pacific (on the west side), and the southeasterly, from the Gulf of Mexico (on the east side). The diurnal variation of the low-level flow can be affected sensitively by simulating the diurnal variations of the synoptic flows (Fig. 8 shows that the southeasterly from the Gulf of the Mexico varies more than the northwesterly from the eastern Pacific).

Our MM5 modeling fails to simulate late evening peak rainfall over the lowest-elevation band. Figure 9 shows the modeled diurnal variability of the mean soundings in July over a coastal site in northern Mexico (28.8°N, 110.6°W; elevation, 389 m). In the morning, there is insufficient convective available potential energy (CAPE) in the atmospheric column to support convective rainfall. From afternoon to the later night, the CAPE above the level of free convection (LFC) reaches values greater than 1000 J kg^{-1}, indicating high buoyant energy forms in the atmosphere column. However, a negative energy layer, the convective inhibition (CIN), exists below the LFC. Under such conditions, the hostile dry layer and CIN make it difficult for convective rainfall to develop. A recent study (Li et al. 2006) using cloud microphysics at a high grid resolution (3 km) shows that this CIN may be diminished by downward outflow from the preceding convection, which occurs over the upper (mountain) slope.

5. Summary

A regional climate model, the MM5, was used to study the capabilities and limitations of simulating characteristics of the 2004 NAM at intraseasonal time

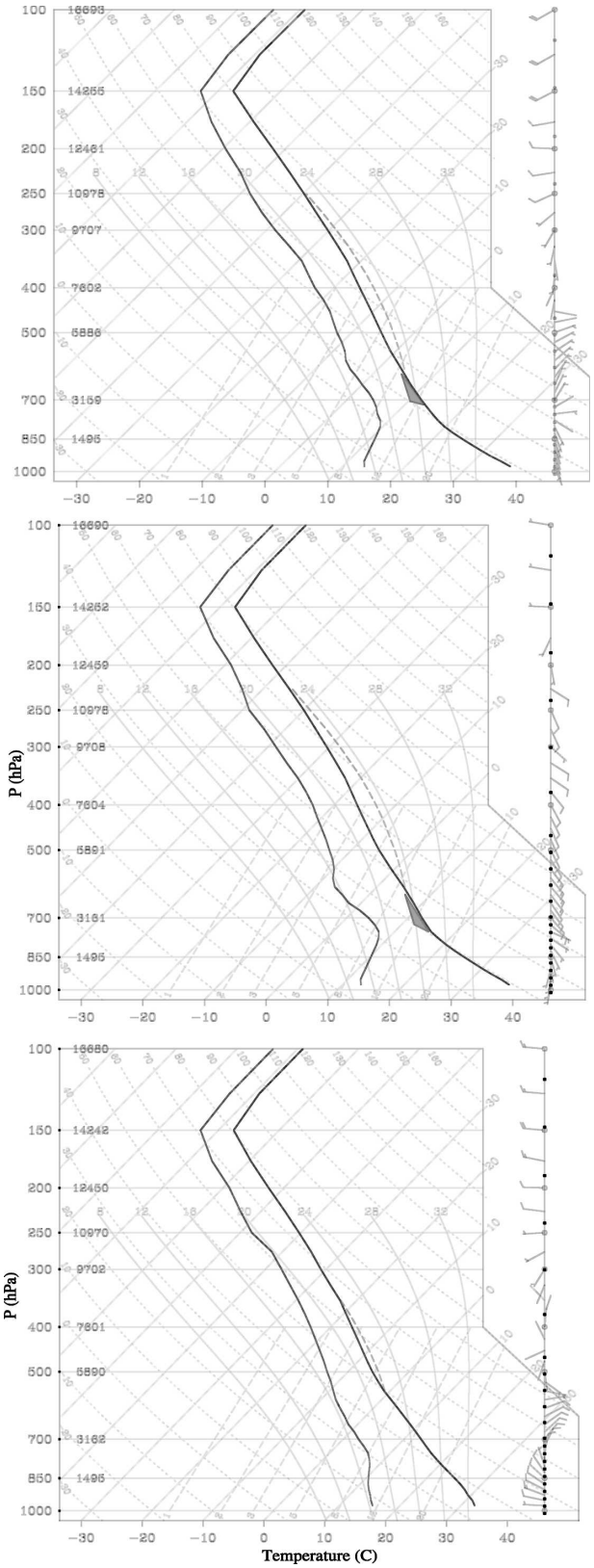

FIG. 9. Modeled mean soundings for July at 2100, 0000, and 0300 UTC over 28.8°N, 110.6°W (elevation, 389 m).

scales. The study domains (NAME tiers 2 and 3) were nested inside the ECMWF global 2.5° analysis system and computed with 75 km × 25 km horizontal grid resolutions and 28 vertical layers. To control modeling errors, the model run was reinitialized every 5 days (with a 12-h spinup run for each initialization), giving the model run a much higher spatial resolution but less frequent internal-grid adjustments than the parent ECMWF analysis system. The model's performance in simulating the 2004 NAM was evaluated according to the major intraseasonal features of NAM precipitation, including the evolution of the NAM precipitation regime, monsoon onset, moisture surge over the Gulf of California, and diurnal variability of monsoon precipitation and low-level flows.

It is encouraging that the model in this case study shows the potential to predict most of the 2004 NAM's intraseasonal characteristics. The modeled results of monthly precipitation variation (over land) and synoptic circulations in time and space describe the beginning, growth, and maturity of the 2004 NAM system, as well as the interaction of the three summertime precipitation regimes over the conterminous United States, which match the observations and are consistent with the diagnostic analyses. However, the model underestimates the monthly rainfall amounts and coverage areas.

The modeled daily precipitation time series at local areas (boxes AZNM, A, B, C, D, and E), though unable to match the observations event by event, shows the monsoon onset and subsequent transitions in dry–wet episodes that agree with the observations. The model precipitation is overestimated over the southwestern United States, and in particular, over the mountainous area of the Mogollon Rim (box A), but underestimated over the western slope of the SMO, northwestern Mexico.

Based on changes in surface dewpoint and meridional winds at Yuma, the model predicted the onset and ending days for the four gulf surges that occurred in July and August. This is because, as shown for surge 1, the model is able to reproduce the surge progression stimulated by strong forcing (Tropical Storm Blas) acting at the mouth of the Gulf of California.

The modeled diurnal patterns of low-level flows indicate that sustaining sea breezes are the source of afternoon to later night rainfall over the western slopes of the SMO. The model displays the migration of convection activity (the convergence line) from the highest-elevation band (mountain peak) to the lowest-elevation band (coast) during the afternoon to late night. However, the modeled diurnal precipitation variability misses the observed corresponding shift in the diurnal rain peak. The model also fails to produce rainfall over the coastal band. This and other precipitation errors suggest that the K–F convective parameterization scheme, which is responsible for the model's precipitation production, needs to be improved. Based on its afternoon and night soundings, we identified the existence of a negative energy layer (CIN) over the costal areas, which blocks the development of convective rainfall in those areas. A recent study (Li et al. 2006) using cloud microphysics at a high grid resolution (3 km) shows that the CIN over the coastal band can be diminished by outflow from the preceding convection that occurs over the upper slope of the SMO.

The diurnal patterns in surface flows also identify two southerly LLJs that reach the southwestern United States with tropical moisture: one in the morning from northern Mexico and another in the afternoon and evening from the northern end of the Gulf of California. However, the model's timing for the maximum LLJ from the Gulf of California disagrees with the observed early morning time.

This study concludes that high variability in precipitation is a pronounced feature of the NAM that is associated with water and energy processes in the system. Model predictions of monsoon precipitation still include errors of quantity, pattern, and timing. Therefore, improving precipitation prediction should be a high priority for the NAME study. Evidence from our study suggests improving the MM5 model's ability to predict precipitation may occur first at intraseasonal time scales.

Acknowledgments. The comments and suggestions provided by three anonymous reviewers were extremely useful and helped the authors to improve this paper. Primary support for this research was provided under the NASA/EOS Interdisciplinary Research Program (NNG04GK35G; NNG05GA20G), the NOAA GAPP Program (NA04OAR4310086), and the NSF–STC Program (Agreement EAR-9876800).

REFERENCES

Adams, D. K., and A. C. Comrie, 1997: The North American monsoon. *Bull. Amer. Meteor. Soc.,* **78,** 2197–2213.

Anderson, B. T., and J. O. Roads, 2002: Regional simulation of summertime precipitation over the southwestern United States. *J. Climate,* **15,** 3321–3342.

——, ——, S.-C. Chen, and H.-M. H. Juang, 2000: Large-scale forcing of summertime monsoon surges over the Gulf of California and the southwestern United States. *J. Geophys. Res.,* **105,** 24 455–24 467.

Barlow, M., S. Nigam, and E. H. Berbery, 1998: Evolution of the North American monsoon system. *J. Climate,* **11,** 2238–2257.

Berbery, E. H., 2001: Mesoscale moisture analysis of the North American monsoon. *J. Climate,* **14,** 121–137.

Bright, D. R., and S. L. Mullen, 2002: The sensitivity of the numerical simulation of the Southwest monsoon boundary layer to the choice of PBL turbulence parameterization in MM5. *Wea. Forecasting,* **17,** 99–114.

Cavazos, T., A. C. Comrie, and D. M. Liverman, 2002: Intraseasonal variability associated with wet monsoons in southeast Arizona. *J. Climate,* **15,** 2477–2490.

Chen, F., and J. Dudhia, 2001: Coupling an advanced land surface hydrology model with the Penn State–NCAR MM5 modeling system. Part I: Model implementation and sensitivity. *Mon. Wea. Rev.,* **129,** 569–585.

Dai, A., F. Giorgi, and K. E. Trenberth, 1999: Observed and model-simulated diurnal cycles of precipitation over the contiguous United States. *J. Geophys. Res.,* **104,** 6377–6402.

Douglas, M. W., and S. Li, 1996: Diurnal variation of the lower-tropospheric flow over the Arizona low desert from SWAMP-1993 observations. *Mon. Wea. Rev.,* **124,** 1211–1235.

——, and J. C. Leal, 2003: Summertime surges over the Gulf of California: Aspects of their climatology, mean structure, and evolution from radiosonde, NCEP reanalysis, and rainfall data. *Wea. Forecasting,* **18,** 55–74.

——, R. A. Maddox, K. Howard, and S. Reyes, 1993: The Mexican monsoon. *J. Climate,* **6,** 1665–1677.

——, A. Valdez-Manzanila, and R. G. Cueta, 1998: Diurnal variation and horizontal extent of the low-level jet over the northern Gulf of California. *Mon. Wea. Rev.,* **126,** 2017–2025.

Dudhia, J., 1989: Numerical study of convection observed during the Winter Monsoon Experiment using a mesoscale two-dimensional model. *J. Atmos. Sci.,* **46,** 3077–3107.

Gao, X., S. Sorooshian, J. Li, and J. Xu, 2003: SST data improve modeling of North American monsoon rainfall. *Eos, Trans. Amer. Geophys. Union,* **84,** P457–P462.

Gochis, D. J., W. J. Shuttleworth, and Z.-L. Yang, 2002: Sensitivity of the modeled North American monsoon regional climate to convective parameterization. *Mon. Wea. Rev.,* **130,** 1282–1298.

——, J. Leal, W. J. Shuttleworth, C. J. Watts, and G. Jaime, 2003: Preliminary diagnostics from a new event-based precipitation monitoring system in support of the North American Monsoon Experiment. *J. Hydrometeor.,* **4,** 974–981.

——, A. Jimenez, C. J. Watts, G. Jaime, and W. J. Shuttleworth, 2004: Analysis of 2002 and 2003 warm-season precipitation from the North American Monsoon Experiment Event Rain Gauge Network. *Mon. Wea. Rev.,* **132,** 2938–2953.

Higgins, R. W., and W. Shi, 2000: Dominant factors responsible for interannual variability of the Southwest monsoon. *J. Climate,* **13,** 759–776.

——, and ——, 2001: Intercomparison of the principal modes of interannual and intraseasonal variability of the North American monsoon system. *J. Climate,* **14,** 403–417.

——, Y. Yao, and X. L. Wang, 1997: Influence of the North American monsoon system on the U.S. summer precipitation regime. *J. Climate,* **10,** 2600–2622.

——, Y. Chen, and A. V. Douglas, 1999: Interannual variability of the North American warm season precipitation regions. *J. Climate,* **12,** 653–680.

——, A. Leetmaa, Y. Xue, and A. Barnston, 2000: Dominant factors influencing the seasonal predictability of U.S. precipitation and surface air temperature. *J. Climate,* **13,** 3994–4017.

——, W. Shi, and C. Hain, 2004: Relationships between Gulf of California moisture surges and precipitation in the southwestern United States. *J. Climate,* **17,** 2983–2997.

Hong, S.-Y., and H.-L. Pan, 1996: Nonlocal boundary layer vertical diffusion in a medium-range forecast model. *Mon. Wea. Rev.,* **124,** 2322–2339.

Hong, Y., K. Hsu, S. Sorooshian, and X. Gao, 2004: Precipitation estimation from remotely sensed information using artificial neural network cloud classification system. *J. Appl. Meteor.,* **43,** 1834–1853.

Hsu, K., X. Gao, S. Sorooshian, and H. V. Gupta, 1997: Precipitation estimation from remotely sensed information using artificial neural networks. *J. Appl. Meteor.,* **36,** 1176–1190.

Janjić, Z. I., 1994: The step-mountain Eta coordinate model: Further developments of the convection, viscous sublayer, and turbulence closure schemes. *Mon. Wea. Rev.,* **122,** 927–945.

Kain, J. S., and J. M. Fritch, 1990: A one-dimensional entraining/detraining plume model and its application in convective parameterization. *J. Atmos. Sci.,* **47,** 2784–2802.

Li, J., X. Gao, R. A. Maddox, and S. Sorooshian, 2004: Model study of evolution and diurnal variations of rainfall in the North American monsoon during June and July 2002. *Mon. Wea. Rev.,* **132,** 2895–2915.

——, ——, ——, and ——, 2005: Sensitivity of North American monsoon rainfall to multisource sea surface temperature in MM5. *Mon. Wea. Rev.,* **133,** 2922–2939.

——, ——, K.-L. Hsu, B. Imam, and S. Sorooshian, 2006: Modeling rainfall diurnal variation of Northern American monsoon core using different spatial resolution. Preprints, *27th Conf. on Hurricanes and Tropical Meteorology,* Monterey, CA, Amer. Meteor. Soc., CD-ROM, 12D.5.

Liang, X., L. Li, K. E. Kunkel, M. Ting, and J. X. L. Wang, 2004: Regional climate model simulation of U.S. precipitation during 1982–2002. Part I: Annual cycle. *J. Climate,* **17,** 3510–3529.

Mesinger, F., and Coauthors, 2005: North American Regional Reanalysis. *Bull. Amer. Meteor. Soc.,* **87,** 343–360.

Mo, K. C., 2000: Intraseasonal modulation of summer precipitation over North America. *Mon. Wea. Rev.,* **128,** 1490–1505.

——, and H. M. H. Juang, 2003: Influence of sea surface temperature anomalies in the Gulf of California on North American monsoon rainfall. *J. Geophys. Res.,* **108,** 4112, doi:10.1029/2002JD002403.

NAME Project Science Team, 2004: North American Monsoon Experiment (NAME): Science and implementation plan. NOAA/NCEP/CPC, 96 pp. [Available online at http://www.cpc.ncep.noaa.gov/products/precip/monsoon/.]

Negri, A. J., R. F. Adler, R. A. Maddox, K. W. Howard, and P. R. Keehn, 1993: A regional rainfall climatology over Mexico and the southwest United States derived from passive microwave and geosynchronous infrared data. *J. Climate,* **6,** 2144–2161.

Ropelewski, C. F., and M. S. Halpert, 1996: Quantifying Southern Oscillation–precipitation relationships. *J. Climate,* **9,** 1043–1059.

Saleeby, M. S., and W. R. Cotton, 2004: Simulation of the North

American monsoon system. Part I: Model analysis of the 1993 monsoon season. *J. Climate,* **17,** 1997–2018.

Sorooshian, S., K. Hsu, X. Gao, H. V. Gupta, B. Imam, and D. Braithwaite, 2000: Evaluation of PERSIANN system satellite–based estimates of tropical rainfall. *Bull. Amer. Meteor. Soc.,* **81,** 2035–2046.

——, X. Gao, K. Hsu, R. A. Maddox, Y. Hong, H. V. Gupta, and B. Iman, 2002: Diurnal variability of tropical rainfall retrieved from combined GOES and TRMM satellite information. *J. Climate,* **15,** 983–1001.

Stensrud, D. J., R. L. Gall, S. L. Mullen, and K. W. Howard, 1995: Model climatology of the Mexican monsoon. *J. Climate,* **8,** 1775–1794.

——, ——, and M. K. Nordquist, 1997: Surges over the Gulf of California during the Mexican monsoon. *Mon. Wea. Rev.,* **125,** 417–437.

Wang, W., and N. L. Seaman, 1997: A comparison study of convective parameterization schemes in a mesoscale model. *Mon. Wea. Rev.,* **125,** 252–278.

Xu, J., X. Gao, J. Shuttleworth, S. Sorooshian, and E. Small, 2004: Model climatology of the North American monsoon onset period during 1980–2001. *J. Climate,* **17,** 3892–3906.

Yu, B., and J. M. Wallace, 2000: The principal mode of interannual variability of the North American monsoon system. *J. Climate,* **13,** 2794–2800.